

Sparse Domain Transfer via Elastic Net Regularization

Jingwei Zhang*, Farzan Farnia†

Abstract

Transportation of samples across different domains is a central task in several machine learning problems. A sensible requirement for domain transfer tasks in computer vision and language domains is the sparsity of the transportation map, i.e., the transfer algorithm aims to modify the least number of input features while transporting samples across the source and target domains. In this work, we propose *Elastic Net Optimal Transport (ENOT)* to address the sparse distribution transfer problem. The ENOT framework utilizes the L_1 -norm and L_2 -norm regularization mechanisms to find a sparse and stable transportation map between the source and target domains. To compute the ENOT transport map, we consider the dual formulation of the ENOT optimization task and prove that the sparsified gradient of the optimal potential function in the ENOT’s dual representation provides the ENOT transport map. Furthermore, we demonstrate the application of the ENOT framework to perform feature selection for sparse domain transfer. We present the numerical results of applying ENOT to several domain transfer problems for synthetic Gaussian mixtures and real image and text data. Our empirical results indicate the success of the ENOT framework in identifying a sparse domain transport map.

1 Introduction

Deep neural networks (DNNs) have revolutionized the performance of computer vision models in domain transfer applications where the features of an input sample are altered to transfer the sample to a secondary domain (Jiang et al., 2020; Ojha et al., 2021; Zhu et al., 2020). The common goal of domain transfer algorithms is to transport an input data point to a target distribution by applying *minimal changes* to the input. Over recent years, domain transportation algorithms based on generative adversarial networks (GANs) including CycleGAN (Zhu et al., 2017) and StyleGAN (Karras et al., 2019) have achieved empirical success in addressing the domain transfer task for image distributions. The success of these algorithms has inspired several studies of GAN-based domain transfer methodologies (Chen et al., 2020; van der Ouderaa and Worrall, 2019; Zhao et al., 2020).

While the GAN-based methods have led to successful results in image-based domain transfer problems, their application demands significantly higher computational costs than standard GAN algorithms including only one generator/discriminator neural net pair to transfer a latent Gaussian vector to the data distribution. The extra computations in these domain transfer algorithms aim to ensure an invertible transfer map and thus limited modifications to an input sample. For example, the CycleGAN algorithm considers two pairs of generator/discriminator neural nets to impose a reversible transformation of an input image. However, the additional pair of neural nets in the CycleGAN setting will lead to a more challenging optimization task and higher training costs.

In this work, we focus on *sparse domain transfer problems* where the transfer of samples between source and target domains can be achieved by editing only a limited subset of input features. We note that the assumption of a sparse transport map applies to several real-world domain transfer problems, e.g. object translation, text revision, and gene editing problems. In the mentioned tasks, the sparsity level of the transfer map results in a meaningful measure of changes applied to an input sample. While sparse transportation

*Department of Computer Science and Engineering, The Chinese University of Hong Kong, jwzhang22@cse.cuhk.edu.hk

†Department of Computer Science and Engineering, The Chinese University of Hong Kong, farnia@cse.cuhk.edu.hk

maps are desired in many real-world domain transfer problems, the commonly-used GAN-based algorithms often lead to dense transfer maps editing a considerable fraction of input features.

To address sparse domain transfer tasks, we propose an optimal transport-based approach which takes advantage of the induced sparsity of the L_1 -norm regularization and the stability properties of the L_2 -norm regularization. Our proposed framework, which we call *Elastic Net Optimal Transport (ENOT)*, solves an optimal transport problem where the transportation cost follows from the elastic net function (Zou and Hastie, 2005) combining standard Euclidean-norm-squared and L_1 -norm cost functions. Therefore, the ENOT approach can be interpreted as a mechanism to regularize the standard optimal transport map toward sparser transportation functions. By tuning the coefficient of the L_1 -norm regularization in ENOT’s elastic net cost, the learner can adjust the sparsity level of the transportation map and explore the spectrum between the standard and fully L_1 -norm-based optimal transport tasks.

To analyze the ENOT problem, we leverage optimal transport theory (Villani et al., 2009) and extend the duality results to the ENOT optimal transport setting. We prove a generalization of standard Brenier’s theorem, highlighting the connection between the optimal potential function in the ENOT’s dual problem with the optimal transport map transferring samples across domains. Our main theorem suggests that the composition of a soft-thresholding function with the gradient of the optimal potential function will perform sparse transportation across the domains. This result indicates that the ENOT framework offers a combination of the standard optimal transport problem with the squared-error cost function and the L_1 -norm-based optimal transport problem which leads to a challenging optimization problem without the L_2 -norm-based regularization in ENOT.

Furthermore, we utilize the ENOT framework to develop a *feature selection-based approach* to reduce the sparse domain transport task to a constraint-free distribution transfer problem where an unconstrained transfer map is applied to only the selected feature subset. According to this variable selection-based approach, we break the domain transfer problem into two sub-problems: 1) ENOT-based variable selection choosing features to undergo modification for a given input sample, 2) Applying an unconstrained transportation map via standard GAN frameworks that transfers the input sample masked by the feature selection output to the target domain. By tuning the coefficient of the L_1 -norm regularization in the ENOT’s elastic net cost, the learner can adjust the number of selected features prior to performing a constraint-free GAN-based distribution transfer.

Finally, we discuss the numerical results of the applications of the ENOT framework to sparse domain transfer problems from various areas including computer vision, computational biology, and natural language processing. Our empirical findings show that the feature selection-based domain transfer via ENOT can be easily adapted to different domains and achieves satisfactory results. We qualitatively evaluate ENOT’s application for feature identification in sparse domain transfer. The numerical results support the proposed methodology of sparse domain transfer via ENOT-based domain transportation and feature selection. The contributions of this work can be summarized as:

- Proposing a feature selection-based approach for the sparse domain transfer problem,
- Developing ENOT as an elastic net-based methodology to the sparse domain transfer and variable selection,
- Extending the theory of standard squared-error-based optimal transport task to the ENOT setting,
- Providing supportive numerical results for applying ENOT-based sparse domain transfer to various domain transfer tasks.

2 Related Work

Sparsity and Optimal Transport Methods. Several related works have studied various notions of sparsity in optimal transport frameworks. References (Bao and Sakaue, 2022; Blondel et al., 2018; Flamaray et al., 2016; Liu et al., 2023; Swanson et al., 2020) propose sparsity-based regularization of the transportation matrix in optimal transport problems. However, we note that the sparsity objective pursued in these

works differs from the sparse domain transfer in our work: while the mentioned papers aim for a sparse transportation matrix to gain a sparse alignment of source and target samples, our proposed ENOT method focuses on the sparsity of the modified input features in the domain transfer.

Cuturi et al. (2023) first introduces an optimal transport-based approach to the sparse domain transfer problem, which aim to precisely solve an entropic-regularized optimal transport problem over the empirical samples and then use a kernel-based interpolation to generalize the solution to unseen data. On the other hand, our approach to the optimal transport problem is different and more similar to the Wasserstein GAN framework, where we leverage a neural net potential function which can be extended to large-scale image and text data. Overall, our neural net-based method for the ENOT optimal transport problem can be viewed as a complementary approach to the precise kernel-based framework in (Cuturi et al., 2023). Also, the trained neural net can be used as an efficient-to-compute feature selection map, which we later used to introduce a *feature selection-based approach* to sparse domain transfer, a topic that has not been studied in (Cuturi et al., 2023), which is useful for large-scale image and text-related applications.

Unsupervised Image to Image Translation (UI2I). Several related works attempt to address image-based transportation problems. For the image style transfer task, CycleGAN (Zhu et al., 2017) uses a cycle-consistent loss and two GANs to conduct cyclic unpaired transformation. DRIT++ (Lee et al., 2020) adopts encoders to obtain the latent representation of images and similar cross-cycle consistency loss. For the image colorization transfer task, Conditional GANs are leveraged to improve colorization performance (Isola et al., 2017). Zhang et al. (2017) propose a real-time user-guided neural network colorization. Moreover, cyclic-loss (Bhattacharjee et al., 2020; Shen et al., 2019; Wu et al., 2019; Zhu et al., 2017) and GANs (Chen et al., 2020; van der Ouderaa and Worrall, 2019; Zhao et al., 2020) have been utilized to address UI2I. However, unlike ENOT, these related works do not focus on the sparsity of transfer maps.

Sequence to Sequence Translation. Sequence to sequence (Seq2Seq) neural net models are typically designed based on an encoder-decoder architecture. Kalchbrenner and Blunsom (2013) propose the application of a convolutional neural network (CNN) as the encoder and a recurrent neural network (RNN) as the decoder. Sutskever et al. (2014) utilize an RNN-based architecture for both the encoder and decoder neural nets. Vaswani et al. (2017) propose a transformer based on multi-head self-attention. BART (Lewis et al., 2019) offers a sequence-to-sequence pretraining solution and adopts a bidirectional encoder similar to BERT (Devlin et al., 2018), and a decoder similar to GPT (Radford et al., 2018). Unlike our proposed ENOT approach, the discussed methods usually result in a dense transportation map. We also note that Seq2Seq and GAN-based transfer methods are almost exclusively used for language and image distributions, respectively.

3 Preliminaries

Consider random vectors $\mathbf{X}, \mathbf{Y} \in \mathbb{R}^d$ with probability distributions P_X, P_Y , respectively. Given n independent samples $\mathbf{x}_1, \dots, \mathbf{x}_n$ from P_X and m independent samples $\mathbf{y}_1, \dots, \mathbf{y}_m$ from P_Y , the goal in the domain transfer problem is to learn a map $\psi : \mathbb{R}^d \rightarrow \mathbb{R}^d$ transporting an input \mathbf{X} from distribution P_X to an output $\psi(\mathbf{X})$ distributed as P_Y , i.e.,

$$\psi(\mathbf{X}) \stackrel{\text{dist}}{=} \mathbf{Y}.$$

Here, $\stackrel{\text{dist}}{=}$ denotes identical probability distributions.

Without any constraint on the map ψ , there exist infinitely many transportation maps resulting in the required identical distributions. To uniquely characterize the transfer map, the optimal transport framework (Villani et al., 2009) seeks to find a map minimizing the expected transportation cost measured based on a cost function $c : \mathbb{R}^d \times \mathbb{R}^d \rightarrow \mathbb{R}$. According to this framework, the transportation map follows from the optimal coupling $\Pi_{X,Y}$, marginally distributed as P_X and P_Y , that is minimizing the expected transportation cost formulated as

$$\text{OT}_c(P_X, P_Y) := \inf_{\substack{\Pi_{X,Y} : \Pi_X = P_X \\ \Pi_Y = P_Y}} \mathbb{E}_{(X,Y) \sim \Pi} [c(\mathbf{X}, \mathbf{Y})].$$

Here, $\text{OT}_c(P_X, P_Y)$ denotes the optimal transport cost between P_X, P_Y . It is well-known that under mild regularity conditions, a deterministic coupling mapping \mathbf{X} to a sample with distribution P_Y exists that solves the above problem. Also, the dual representation of the above optimization problem can be formulated via the Kantorovich duality (Villani et al., 2009) as

$$\sup_{\phi: \mathbb{R}^d \rightarrow \mathbb{R}} \mathbb{E}[\phi(\mathbf{X})] - \mathbb{E}[\phi^c(\mathbf{Y})],$$

where ϕ is the potential function and the c -transform ϕ^c is defined as $\phi^c(\mathbf{y}) := \sup_{\mathbf{y}' } \phi(\mathbf{y}') - c(\mathbf{y}, \mathbf{y}')$.

Example 1. In the special case of a norm cost $c_1(\mathbf{x}, \mathbf{y}) = \|\mathbf{x} - \mathbf{y}\|$, the result of Kantorovich duality can be written as

$$\text{OT}_{c_1}(P_X, P_Y) = \sup_{\phi: 1\text{-Lipschitz}} \mathbb{E}[\phi(\mathbf{X})] - \mathbb{E}[\phi(\mathbf{Y})]$$

where the potential function $\phi: \mathbb{R}^d \rightarrow \mathbb{R}$ is constrained to be 1-Lipschitz with respect to the assigned norm $\|\cdot\|$, i.e., for every $\mathbf{x}, \mathbf{x}' \in \mathbb{R}^d$:

$$|\phi(\mathbf{x}) - \phi(\mathbf{x}')| \leq \|\mathbf{x} - \mathbf{x}'\|.$$

Example 2. In the special case of the L_2 -norm-squared cost $c_2(\mathbf{x}, \mathbf{y}) = \frac{1}{2}\|\mathbf{x} - \mathbf{y}\|_2^2$, the result of Kantorovich duality can be written as

$$\sup_{\tilde{\phi}: \text{convex}} \mathbb{E}\left[\frac{1}{2}\|\mathbf{X}\|_2^2 - \tilde{\phi}(\mathbf{X})\right] + \mathbb{E}\left[\frac{1}{2}\|\mathbf{Y}\|_2^2 - \tilde{\phi}^*(\mathbf{Y})\right] \quad (1)$$

where the potential function $\phi(\mathbf{x}) := \frac{1}{2}\|\mathbf{x}\|_2^2 - \tilde{\phi}(\mathbf{x})$ is constrained to be the subtraction of a convex function $\tilde{\phi}$ from $\frac{1}{2}\|\mathbf{x}\|_2^2$, and $\tilde{\phi}^*$ is the Fenchel conjugate defined as

$$\tilde{\phi}^*(\mathbf{x}) := \sup_{\mathbf{x}'} \mathbf{x}'^\top \mathbf{x} - \tilde{\phi}(\mathbf{x}').$$

The Brenier theorem reveals that in the setting of Example 2, the gradient of the optimal solution $\tilde{\phi}$ provides the unique monotone (gradient of a convex function) map transporting samples between the two domains:

Theorem 1 (Brenier's Theorem, (Villani et al., 2009)). *Suppose that P_X, P_Y are absolutely continuous with respect to one another. Then, the gradient of the solution $\tilde{\phi}^*$ to equation 1 is the unique monotone map for transferring P_X to P_Y , that is*

$$\nabla \tilde{\phi}^*(\mathbf{X}) \stackrel{\text{dist}}{=} \mathbf{Y}.$$

In the following sections, we aim to define and analyze optimal transport costs that can capture the sparsity of the transportation map, i.e. the number of non-zero coordinates of $\mathbf{y} - \mathbf{x}$.

4 Elastic Net Regularization for Sparse Optimal Transport

In this work, we aim to address the sparse domain transfer problem where the transfer map ψ between distributions P_X, P_Y alters the fewest possible coordinates in the d -dimensional feature vector $\mathbf{X} = [X^{(1)}, \dots, X^{(d)}]$. To apply the optimal transport framework, a proper cost function is the cardinality (number of non-zero elements $\text{card}(\mathbf{z}) = \sum_{i=1}^d \mathbf{1}[z_i \neq 0]$) of the difference between the original and transported samples:

$$c_{\text{sparse}}(\mathbf{x}, \mathbf{y}) = \text{card}(\mathbf{x} - \mathbf{y}).$$

Since the cardinality function lacks continuity and convexity, the resulting optimal transport problem will be computationally difficult. A common convex proxy for the cardinality function is the L_1 -norm where we simply use $c_{L_1}(\mathbf{x}, \mathbf{y}) = \|\mathbf{x} - \mathbf{y}\|_1$. While the primal optimal transport problem could be solved for the empirical

samples with the L_1 -norm cost, the domain transfer map requires solving the optimization problem for the data distribution which would be complex in the primal case. Therefore, we focus on the dual optimization problem to the optimal transport task. However, solving the dual optimization problem of the L_1 -norm cost requires optimizing over the L_1 -norm-based 1-Lipschitz functions which would be challenging.

To handle the computational complexity of the dual optimization problem with L_1 -norm cost function, we propose to apply the *elastic net* (Zou and Hastie, 2005) cost function with coefficients $0 \leq \alpha \leq 1$ and $\lambda > 0$:

$$c_{\text{EN}}^{\alpha, \lambda}(\mathbf{x}, \mathbf{y}) = \lambda(1 - \alpha)\|\mathbf{x} - \mathbf{y}\|_2^2 + \lambda\alpha\|\mathbf{x} - \mathbf{y}\|_1. \quad (2)$$

Using the above cost function, we propose the *Elastic Net-based Optimal Transport (ENOT)* as the optimal transport method formulated with the cost function in equation 2. For the dual formulation of the ENOT problem, we can apply the Kantorovich duality to obtain the following optimization task:

$$\max_{\phi: \mathbb{R}^d \rightarrow \mathbb{R}} \mathbb{E}[\phi(\mathbf{X})] - \mathbb{E}[\phi^{c_{\text{EN}}^{\alpha, \lambda}}(\mathbf{Y})] \quad (3)$$

where the elastic-net-based c -transform can be written as follows:

$$\phi^{c_{\text{EN}}^{\alpha, \lambda}}(\mathbf{y}) := \max_{\boldsymbol{\delta} \in \mathbb{R}^d} \phi(\mathbf{y} + \boldsymbol{\delta}) - \lambda(1 - \alpha)\|\boldsymbol{\delta}\|_2^2 - \lambda\alpha\|\boldsymbol{\delta}\|_1.$$

Theorem 2. *Consider the ENOT dual problem in equation 3. Then, there exists an optimal potential function ϕ^* for this problem which satisfies the following weakly-concavity property: for every $\mathbf{x}, \mathbf{y} \in \mathbb{R}^d$ and real value $\gamma \in [0, 1]$:*

$$\phi^*(\gamma\mathbf{x} + (1 - \gamma)\mathbf{y}) \geq \gamma\phi^*(\mathbf{x}) + (1 - \gamma)\phi^*(\mathbf{y}) - \lambda\gamma(1 - \gamma)(1 - \alpha)\|\mathbf{x} - \mathbf{y}\|_2^2 - \lambda\alpha\|\mathbf{x} - \mathbf{y}\|_1.$$

Proof. We defer the proof to the Appendix. □

The above result shows the existence of an optimal potential function possessing a weakly-concave structure defined based on an elastic net function. Our next result reveals the extension of the Brenier's theorem to the elastic net cost function. In this extension, we use ST_γ to denote the soft-thresholding operator defined for a scalar input as

$$\text{ST}_\gamma(z) := \begin{cases} z + \gamma & \text{if } z \leq -\gamma \\ 0 & \text{if } -\gamma < z < \gamma \\ z - \gamma & \text{if } \gamma \leq z. \end{cases}$$

For a vector input $\mathbf{z} \in \mathbb{R}^d$, we define the soft-thresholding map as the coordinate-wise application of the scalar soft-thresholding function, i.e.,

$$\forall i \in \{1, \dots, d\}: \quad \text{ST}_\gamma(\mathbf{z})_i = \text{ST}_\gamma(z_i)$$

Theorem 3. *Consider the dual ENOT problem in equation 3. Then, given the optimal potential function ϕ^* the following will provide the optimal transport map transferring samples across domains:*

$$\mathbf{X} - \text{ST}_{\frac{\alpha}{2(1-\alpha)}}\left(\frac{1}{2\lambda(1-\alpha)}\nabla\phi^*(\mathbf{X})\right) \stackrel{\text{dist}}{=} \mathbf{Y}.$$

Proof. We defer the proof to the Appendix. □

Note that the above theorem is a generalization of the Brenier theorem for the elastic net cost, and in the special case of $\alpha = 0$ reduces to the Brenier theorem. On the other hand, by selecting a larger L_1 -regularization coefficient α , the soft-thresholding map will apply a more stringent sparsification to the gradient map of the optimal potential function. This result suggests that by choosing a larger α , one can achieve a sparser transportation map which is the goal sought by the sparse transfer algorithm. Theorem 3 reduces the search for the elastic net-based transport map to the computation of the optimal potential function ϕ in the dual optimization problem, which as shown in Theorem 2 satisfies a weakly-concavity property.

Table 1: ENOT’s achieved NLL with different coefficients of L_1 -regularization on the Gaussian mixture transfer.

f	dimension	ENOT L_1 coefficient						
		baseline 0	1e-3	5e-3	1e-2	5e-2	1e-1	5e-1
MLP-22	1000	4.87×10^3	4.46×10^3	4.13×10^3	3.52×10^3	1.50×10^3	1.50×10^3	1.51×10^3
	100	3.22×10^3	3.15×10^3	2.97×10^3	1.82×10^3	1.62×10^2	1.64×10^2	1.82×10^2
	10	1.53×10^1	1.50×10^1	1.42×10^1	1.39×10^1	1.31×10^1	1.40×10^1	1.51×10^1
MLP-12	1000	4.56×10^3	4.42×10^3	4.02×10^3	3.48×10^3	1.50×10^3	1.50×10^3	1.50×10^3
	100	2.73×10^3	2.58×10^3	2.85×10^3	1.27×10^3	1.50×10^2	1.51×10^2	1.51×10^2
	10	1.60×10^1	1.39×10^1	1.51×10^1	1.48×10^1	1.34×10^1	1.48×10^1	1.67×10^1
MLP-4	1000	3.67×10^3	3.62×10^3	3.44×10^3	3.01×10^3	1.50×10^3	1.50×10^3	1.50×10^3
	100	2.62×10^3	2.53×10^3	1.44×10^3	1.01×10^3	1.50×10^2	1.51×10^2	1.51×10^2
	10	1.52×10^1	1.36×10^1	1.38×10^1	1.44×10^1	1.32×10^1	1.47×10^1	1.77×10^1

5 ENOT-based Feature Selection for Sparse Domain Transfer

In the previous section, we have shown sparse transfer map could be derived by applying the soft-thresholding function to the gradient of the optimal potential function. In addition to directly performing a sparse optimal transport, the trained potential function in the ENOT framework can be used for variable selection to undergo an unconstrained distribution transfer. Therefore, we also propose a feature selection algorithm for domain transfer using the optimal potential function ϕ^* in equation 3. Here for an input $\mathbf{x} \in \mathbb{R}^d$, we define the feature selection mask $I : \mathbb{R}^d \rightarrow \{0, 1\}^d$ as

$$\forall i \in \{1, \dots, d\} : I(\mathbf{x})_i = \begin{cases} 0 & \text{if } |\nabla \phi^*(\mathbf{x})_i| \leq \lambda \alpha, \\ 1 & \text{if } |\nabla \phi^*(\mathbf{x})_i| > \lambda \alpha \end{cases} \quad (4)$$

The above masking identifies the feature coordinates modified by the ENOT transport map. Given the above masking function, we can train a generator function $G : \mathbb{R}^d \rightarrow \mathbb{R}^d$ to perform a constraint-free domain transportation on the ENOT’s selected features. We can employ the standard GAN framework (Goodfellow et al., 2014) consisting of a generator G and discriminator function $D : \mathbb{R}^d \rightarrow \mathbb{R}$ to do this task. Following the standard min-max formulation of GANs, we propose the following optimization problem for the ENOT feature selection-based domain transport:

$$\min_{G \in \mathcal{G}} \max_{D \in \mathcal{D}} \mathbb{E} \left[\log(D(\mathbf{Y})) \right] + \mathbb{E} \left[\log \left(1 - D \left(I(\mathbf{X}) \odot G(\mathbf{X}) + (1 - I(\mathbf{X})) \odot \mathbf{X} \right) \right) \right]$$

In the above, the generator G attempts to match the distribution of modified $I(\mathbf{X}) \odot G(\mathbf{X}) + (1 - I(\mathbf{X})) \odot \mathbf{X}$ with the distribution of \mathbf{Y} , where \odot denotes the element-wise Hadamard product. On the other hand, the discriminator D seeks to identify the original \mathbf{Y} samples from the modified \mathbf{X} data. Since we utilize the feature selection mask of the trained ENOT potential function, we do not need to ensure the invertibility of the generator and can reduce the number of machine players compared to the CycleGAN algorithm.

The above feature selection-based approach enables the application of neural net generator functions which could improve the vanilla ENOT’s performance due to the power of a properly-designed generator to model the structures in the text and image data. This is similar to the Wasserstein GAN (WGAN) (Arjovsky et al., 2017) as the optimal-transport-based GAN formulation in WGANs also considers a generator G instead of relying on the gradient of the potential function.

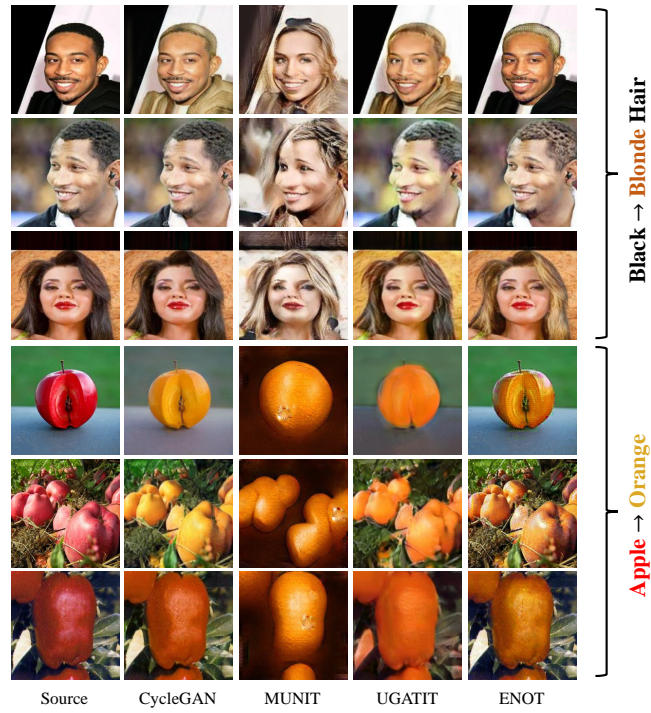


Figure 1: Transportation for Black to Blonde hair and Apple to Orange on CelebA and Apple2Orange.

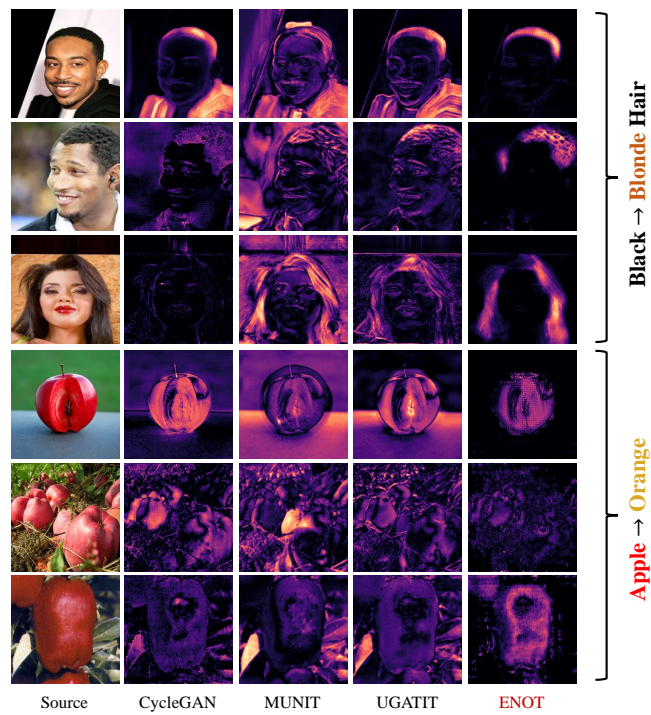


Figure 2: Saliency maps of transportation for Black to Blonde hair and Apple to Orange on CelebA and Apple2Orange.

6 Numerical Results

In this section, we present the empirical results of the applications of ENOT and the baseline domain transfer algorithms to several standard datasets, including synthetic Gaussian mixture models, and real image and text datasets. We defer the details of our numerical experiments, including the dataset pre-processing, neural network architectures, and hyperparameter selection to the Appendix.

6.1 ENOT applied to Synthetic Gaussian Mixture Data

We evaluated the performance of ENOT in domain transfer problems across multivariate Gaussian mixture models (GMMs). In our experiments, we considered bimodal source and target GMMs: the source GMM $p(\mathbf{x}) = \phi_s \mathcal{N}(\mathbf{x} | \boldsymbol{\mu}_s, \sigma^2 \mathbf{I}_d) + (1 - \phi_s) \mathcal{N}(\mathbf{x} | -\boldsymbol{\mu}_s, \sigma^2 \mathbf{I}_d)$, and target GMM $p(\mathbf{y}) = \phi_t \mathcal{N}(\mathbf{y} | \boldsymbol{\mu}_t, \sigma^2 \mathbf{I}_d) + (1 - \phi_t) \mathcal{N}(\mathbf{y} | -\boldsymbol{\mu}_t, \sigma^2 \mathbf{I}_d)$ both consist of two multivariate Gaussian components with different means and identical covariance matrix with $\sigma = 1$. There exist two component-based mappings: (1) mapping $\mathcal{N}_{\boldsymbol{\mu}_s} \rightarrow \mathcal{N}_{\boldsymbol{\mu}_t}, \mathcal{N}_{-\boldsymbol{\mu}_s} \rightarrow \mathcal{N}_{-\boldsymbol{\mu}_t}$ or (2) mapping $\mathcal{N}_{\boldsymbol{\mu}_s} \rightarrow \mathcal{N}_{-\boldsymbol{\mu}_t}, \mathcal{N}_{-\boldsymbol{\mu}_s} \rightarrow \mathcal{N}_{\boldsymbol{\mu}_t}$. We set $\boldsymbol{\mu}_s = [\gamma, \epsilon_d, \dots, \epsilon_d]$, $\boldsymbol{\mu}_t = [-\gamma, \epsilon_d, \dots, \epsilon_d]$ and chose $\epsilon_d \cdot \sqrt{d} - 1 < \gamma$ to distinguish the optimal L_1 -norm-based sparse and standard L_2 -norm-based transfer maps. We set $\gamma = 10$, $\epsilon_{10} = 2$, $\phi_s = \phi_t = 0.5$, and scaled $\epsilon_d = \frac{\epsilon_{10}}{\sqrt{d/10}}$ to ensure the inequality holds in different dimensions.

We applied the ENOT approach by solving the dual optimization problem (Eq. 3) using a multi-layer perception neural net with different number of ReLU layers. We attempted different L_1 -norm coefficients, where a zero coefficient reduces to the standard optimal transport baseline. We evaluated the performance of the domain transfer algorithm using the averaged negative log-likelihood (NLL) of transferred samples with respect to the target Gaussian mixture distribution. Based on our quantitative results in Table 1, we observed that the ENOT’s sparse transfer maps led to better performance scores for the three potential function architectures.

6.2 Image-based Domain Transfer

We utilized the proposed ENOT framework to perform image domain transfer and compared its performance with baselines: CycleGAN (Zhu et al., 2017), MUNIT (Huang et al., 2018), and UGATIT (Kim et al., 2020). In our computer vision experiments, we used three standard datasets: MNIST (LeCun, 1998), CelebA (Liu et al., 2015) and Apple2Orange (Zhu et al., 2017). For training the ENOT’s potential function, we used a 5-layer MLP in the MNIST experiments and used a Vision Transformer (ViT-base) model with patch size 16 from (Dosovitskiy et al., 2020). We defer the discussion on the selection of the α, λ coefficients we performed in the ENOT-based feature selection to the Appendix.

The object translation task in a computer vision setting typically results in a sparse domain transfer task. For example, if we wish to change the hair color of a human, only partial pixels regarding hair are expected to be modified. In computer vision domain transfer problems, the standard domain transfer algorithms leverage high-capacity GANs to reach satisfactory visual quality. However, in GANs, the goal of the generator is to fool the discriminator. This goal might lead to suboptimal results. For example, in Figure 1, when change the hair color from black to blonde for an individual wearing black clothes, the GAN-based methods could mistakenly alter the color of the clothes to yellow simultaneously, thereby outputting a realistic but overly-changed sample. In this case, sparsity is desired. However, integrating the sparsity prior to the GAN optimization could lead to highly challenging min-max optimization tasks.

In Figure 1, we present the empirical results for randomly selected CelebA samples in the transport task: black hair \rightarrow blonde hair, and Apple2Orange samples in the transport task: apple \rightarrow orange. We observe that transportation maps from the baseline methods are unsatisfactory in several sparse-transportation cases. Two common types of failures are present in Figure 1. The first one is over-transportation, where unnecessary pixels are modified. This is commonly observed in baseline methods which employ dense-transportation algorithms. The second failure is insignificant transportation since baselines are not sensitive enough to the sparse transportation regions. On the other hand, by using ENOT-based feature selection, the transfer

Table 2: IMDB Movie Review Sentiment Transportation Maps

Transfer Task: Negative Review \rightarrow Positive Review		
Red: ENOT’s Selected Words for Domain Transfer. Blue: Modified Parts		
Source	Baseline Seq2Seq	ENOT
Lonely, disconnected, middle-class housewife in the midst of a divorce seeks solace to reflect on her immediate future. at some sort of bed and breakfast by (well, literally in the sea) the ocean that for some sort of odd reason she subs for the owner. enter lonely, arrogant richard gere. he is a plastic surgeon. he is the only guest at the inn in the sea. Diane lane is the lonely housewife. you’ll never guess these two fall immediately in love. a tropical storm makes them true lovers. the subplots in this melodrama make little or no sense. the locations, photography are fine. Gere remains one of the most over-rated actors in cinema and does not disappoint. ms. lane must’ve needed the money, but phones in her part with grace.	Ambitious, determined, middle-class housewife in the midst of a transformative journey seeks inspiration to chart her new path. She finds herself at a charming bed and breakfast right by the beautiful ocean, where she unexpectedly steps in to help the owner. Then, enter the charismatic Richard Gere, a skilled plastic surgeon and the only guest at this idyllic seaside inn. Diane Lane portrays the captivating housewife. You’ll be pleasantly surprised as these two form an instant and profound connection. A tropical storm adds a touch of magic to their love story. The various subplots in this heartfelt drama weave together seamlessly. The stunning locations and photography enhance the overall experience. Gere continues to be one of the most respected actors in cinema, delivering a stellar performance as always.	Lonely, disconnected, middle-class housewife in the midst of a divorce seeks solace to reflect on her immediate future. at some sort of bed and breakfast by (well, literally in the sea) the ocean that for some sort of odd reason she subs for the owner. enter lonely, charismatic richard gere. he is a plastic surgeon. he is the only guest at the inn in the sea. Diane lane is the lonely housewife. you’ll never guess these two fall immediately in love. a tropical storm makes them true lovers. the subplots add depth and intrigue to this melodrama. the breathtaking locations, stunning photography are absolutely remarkable. Gere proves once again that he is one of the most respected actors in the world of cinema and does a fantastic job. ms. lane must’ve needed the money, and delivers her part with grace.

results are considerably improved. As shown in Figure 2, the ENOT feature selection successfully identified the pixels corresponding to the subject’s hair in CelebA and the apples in Apple2Orange samples. The proper variable selection led to a more meaningful domain transfer in these computer vision applications.

6.3 IMDB Review Sentiment Reversal

In addition to image data, we evaluated the performance of ENOT in application to text data. We performed the numerical experiments on the IMDB movie review dataset (Maas et al., 2011). This dataset contains 50,000 movie reviews with positive and negative categories. We defined the transportation task as modifying part of the words to flip the review’s sentiment: negative to positive reviews. We attempted a sparse domain transfer task in this case, as the sparsity level could be a sensible quantification of the revision made to the text data. We expect that a sparse transport map exists in this case, when the transfer map only flips the negative and positive adjectives in the text.

We used ENOT to perform domain transfer in this text-based setting. For the potential function in (Eq. 3), we finetuned a pre-trained BERT transformer (Devlin et al., 2018). As the baseline, we considered a pre-trained Seq2Seq model GPT-3 (Brown et al., 2020). Table 2 shows the empirical results of the baseline and ENOT on a randomly selected sample. For this sample, we observed the revision made with the ENOT-based

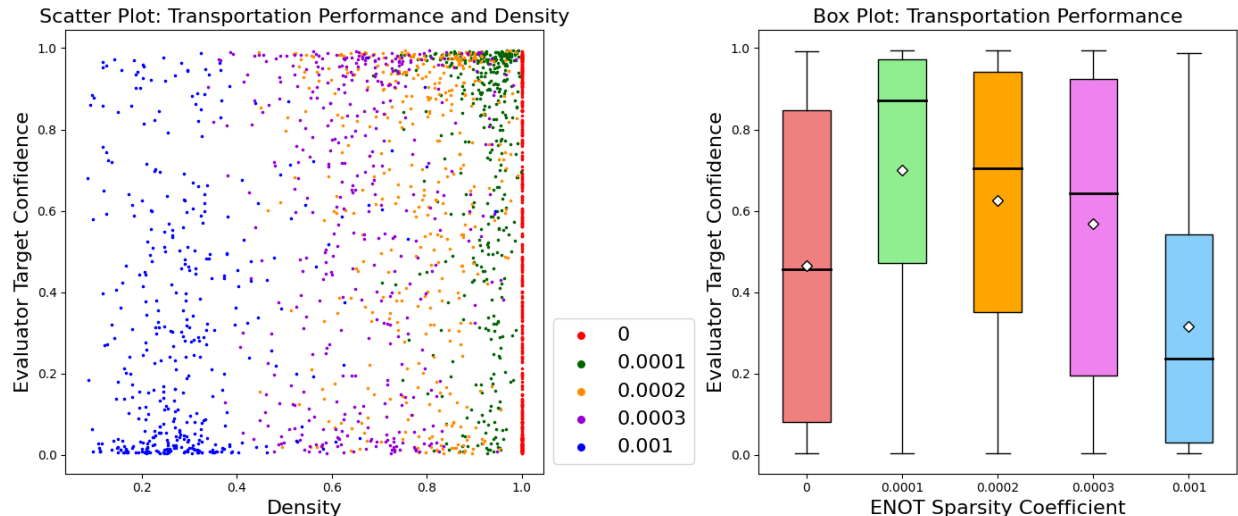


Figure 3: **Left:** IMDB sentiment transfer quality and density. Every point represents a transported sample: color indicates the L_1 -coefficient in ENOT. The x vs. y axes are the transportation quality vs. density. **Right:** Transportation quality, the middle line and diamond show the median and mean. The green bar (coefficient $1e^{-4}$) achieves the highest score.

feature selection method is sparse and only a few words regarding movie review sentiment are modified. In contrast, the baseline Seq2Seq model GPT-3 modified almost all the text, including sentences describing the movie details that sound unrelated to the review sentiment. We present the results for more samples in the Appendix.

Also, we empirically observed that informative words in the generated sparse transportation maps by ENOT have higher correlations with the sentiment compared with other parts of the input text. We present this phenomenon in Figure 3, where we quantified the transportation performance using the confidence score (Mandelbaum and Weinshall, 2017) from a pre-trained BERT model (Devlin et al., 2018) on IMDB sentiment classification. We analyzed the correlation between performance and sparsity in the ENOT’s transportation. In the scatter plot, each point is a random transported sample: the bottom-left region indicates sparse and poor performance, and the top-right region suggests dense and good performance. The box plot statistics in Figure 3 show that a sparsity coefficient of 10^{-4} attains the best performance compared to the dense baseline and other coefficients.

7 Conclusion

In this work, we focused on the sparse domain transfer task and attempted to apply L_1 -norm regularization to the standard optimal transport framework by considering an elastic net cost function. Our numerical results suggest the proposed method’s performance gain under a sparse transfer map. An interesting future direction is to apply the proposed framework to the latent space of image and text data where tighter sparsity constraints may hold in the learning setting. The extension of the elastic net-based optimal transport framework to provide a sparse and concise interpretation of domain transfer maps is another direction for future exploration.

References

- Martin Arjovsky, Soumith Chintala, and Léon Bottou. Wasserstein generative adversarial networks. In *International conference on machine learning*, pages 214–223. PMLR, 2017.
- Han Bao and Shinsaku Sakaue. Sparse regularized optimal transport with deformed q-entropy. *Entropy*, 24(11):1634, 2022.
- Deblina Bhattacharjee, Seungryong Kim, Guillaume Vizier, and Mathieu Salzmann. Dunit: Detection-based unsupervised image-to-image translation. In *Proceedings of the IEEE/CVF Conference on Computer Vision and Pattern Recognition*, pages 4787–4796, 2020.
- Mathieu Blondel, Vivien Seguy, and Antoine Rolet. Smooth and sparse optimal transport. In *International conference on artificial intelligence and statistics*, pages 880–889. PMLR, 2018.
- Stephen P Boyd and Lieven Vandenbergh. *Convex optimization*. Cambridge university press, 2004.
- Tom Brown, Benjamin Mann, Nick Ryder, Melanie Subbiah, Jared D Kaplan, Prafulla Dhariwal, Arvind Neelakantan, Pranav Shyam, Girish Sastry, Amanda Askell, et al. Language models are few-shot learners. *Advances in neural information processing systems*, 33:1877–1901, 2020.
- Runfa Chen, Wenbing Huang, Binghui Huang, Fuchun Sun, and Bin Fang. Reusing discriminators for encoding: Towards unsupervised image-to-image translation. In *Proceedings of the IEEE/CVF conference on computer vision and pattern recognition*, pages 8168–8177, 2020.
- Marco Cuturi, Michal Klein, and Pierre Ablin. Monge, bregman and occam: Interpretable optimal transport in high-dimensions with feature-sparse maps. *arXiv preprint arXiv:2302.04065*, 2023.
- Ugur Demir and Gozde Unal. Patch-based image inpainting with generative adversarial networks. *arXiv preprint arXiv:1803.07422*, 2018.
- Li Deng. The mnist database of handwritten digit images for machine learning research [best of the web]. *IEEE signal processing magazine*, 29(6):141–142, 2012.
- Jacob Devlin, Ming-Wei Chang, Kenton Lee, and Kristina Toutanova. Bert: Pre-training of deep bidirectional transformers for language understanding. *arXiv preprint arXiv:1810.04805*, 2018.
- Alexey Dosovitskiy, Lucas Beyer, Alexander Kolesnikov, Dirk Weissenborn, Xiaohua Zhai, Thomas Unterthiner, Mostafa Dehghani, Matthias Minderer, Georg Heigold, Sylvain Gelly, et al. An image is worth 16x16 words: Transformers for image recognition at scale. *arXiv preprint arXiv:2010.11929*, 2020.
- Rémi Flamary, Nicholas Courty, Davis Tuia, and Alain Rakotomamonjy. Optimal transport for domain adaptation. *IEEE Trans. Pattern Anal. Mach. Intell.*, 1(1-40):2, 2016.
- Todd R Golub, Donna K Slonim, Pablo Tamayo, Christine Huard, Michelle Gaasenbeek, Jill P Mesirov, Hilary Coller, Mignon L Loh, James R Downing, Mark A Caligiuri, et al. Molecular classification of cancer: class discovery and class prediction by gene expression monitoring. *science*, 286(5439):531–537, 1999.
- Ian Goodfellow, Jean Pouget-Abadie, Mehdi Mirza, Bing Xu, David Warde-Farley, Sherjil Ozair, Aaron Courville, and Yoshua Bengio. Generative adversarial nets. *Advances in neural information processing systems*, 27, 2014.
- Xun Huang, Ming-Yu Liu, Serge Belongie, and Jan Kautz. Multimodal unsupervised image-to-image translation. In *ECCV*, 2018.

- Phillip Isola, Jun-Yan Zhu, Tinghui Zhou, and Alexei A Efros. Image-to-image translation with conditional adversarial networks. In *Proceedings of the IEEE conference on computer vision and pattern recognition*, pages 1125–1134, 2017.
- Liming Jiang, Changxu Zhang, Mingyang Huang, Chunxiao Liu, Jianping Shi, and Chen Change Loy. Tsit: A simple and versatile framework for image-to-image translation. In *Computer Vision–ECCV 2020: 16th European Conference, Glasgow, UK, August 23–28, 2020, Proceedings, Part III 16*, pages 206–222. Springer, 2020.
- Nal Kalchbrenner and Phil Blunsom. Recurrent continuous translation models. In *Proceedings of the 2013 conference on empirical methods in natural language processing*, pages 1700–1709, 2013.
- Tero Karras, Samuli Laine, and Timo Aila. A style-based generator architecture for generative adversarial networks. In *Proceedings of the IEEE/CVF conference on computer vision and pattern recognition*, pages 4401–4410, 2019.
- Junho Kim, Minjae Kim, Hyeonwoo Kang, and Kwanghee Lee. U-gat-it: Unsupervised generative attentional networks with adaptive layer-instance normalization for image-to-image translation, 2020.
- Yann LeCun. The mnist database of handwritten digits. <http://yann.lecun.com/exdb/mnist/>, 1998.
- Hsin-Ying Lee, Hung-Yu Tseng, Qi Mao, Jia-Bin Huang, Yu-Ding Lu, Maneesh Singh, and Ming-Hsuan Yang. Drit++: Diverse image-to-image translation via disentangled representations. *International Journal of Computer Vision*, 128:2402–2417, 2020.
- Mike Lewis, Yinhan Liu, Naman Goyal, Marjan Ghazvininejad, Abdelrahman Mohamed, Omer Levy, Ves Stoyanov, and Luke Zettlemoyer. Bart: Denoising sequence-to-sequence pre-training for natural language generation, translation, and comprehension. *arXiv preprint arXiv:1910.13461*, 2019.
- Tianlin Liu, Joan Puigcerver, and Mathieu Blondel. Sparsity-constrained optimal transport. In *The Eleventh International Conference on Learning Representations*, 2023.
- Ziwei Liu, Ping Luo, Xiaogang Wang, and Xiaoou Tang. Deep learning face attributes in the wild. In *Proceedings of International Conference on Computer Vision (ICCV)*, December 2015.
- Andrew L. Maas, Raymond E. Daly, Peter T. Pham, Dan Huang, Andrew Y. Ng, and Christopher Potts. Learning word vectors for sentiment analysis. In *Proceedings of the 49th Annual Meeting of the Association for Computational Linguistics: Human Language Technologies*, pages 142–150, Portland, Oregon, USA, June 2011. Association for Computational Linguistics.
- Amit Mandelbaum and Daphna Weinshall. Distance-based confidence score for neural network classifiers, 2017.
- Utkarsh Ojha, Yijun Li, Jingwan Lu, Alexei A Efros, Yong Jae Lee, Eli Shechtman, and Richard Zhang. Few-shot image generation via cross-domain correspondence. In *Proceedings of the IEEE/CVF Conference on Computer Vision and Pattern Recognition*, pages 10743–10752, 2021.
- Alec Radford, Karthik Narasimhan, Tim Salimans, Ilya Sutskever, et al. Improving language understanding by generative pre-training. 2018.
- Zhiqiang Shen, Mingyang Huang, Jianping Shi, Xiangyang Xue, and Thomas S Huang. Towards instance-level image-to-image translation. In *Proceedings of the IEEE/CVF conference on computer vision and pattern recognition*, pages 3683–3692, 2019.
- Ilya Sutskever, Oriol Vinyals, and Quoc V Le. Sequence to sequence learning with neural networks. *Advances in neural information processing systems*, 27, 2014.

- Kyle Swanson, Lili Yu, and Tao Lei. Rationalizing text matching: Learning sparse alignments via optimal transport. *arXiv preprint arXiv:2005.13111*, 2020.
- Tycho FA van der Ouderaa and Daniel E Worrall. Reversible gans for memory-efficient image-to-image translation. In *Proceedings of the IEEE/CVF Conference on Computer Vision and Pattern Recognition*, pages 4720–4728, 2019.
- Ashish Vaswani, Noam Shazeer, Niki Parmar, Jakob Uszkoreit, Llion Jones, Aidan N Gomez, Lukasz Kaiser, and Illia Polosukhin. Attention is all you need. *Advances in neural information processing systems*, 30, 2017.
- Cédric Villani et al. *Optimal transport: old and new*, volume 338. Springer, 2009.
- Wayne Wu, Kaidi Cao, Cheng Li, Chen Qian, and Chen Change Loy. Transgaga: Geometry-aware unsupervised image-to-image translation. In *Proceedings of the IEEE/CVF conference on computer vision and pattern recognition*, pages 8012–8021, 2019.
- Richard Zhang, Jun-Yan Zhu, Phillip Isola, Xinyang Geng, Angela S Lin, Tianhe Yu, and Alexei A Efros. Real-time user-guided image colorization with learned deep priors. *arXiv preprint arXiv:1705.02999*, 2017.
- Yihao Zhao, Ruihai Wu, and Hao Dong. Unpaired image-to-image translation using adversarial consistency loss. In *ECCV*, 2020.
- Jun-Yan Zhu, Taesung Park, Phillip Isola, and Alexei A Efros. Unpaired image-to-image translation using cycle-consistent adversarial networks. In *Proceedings of the IEEE international conference on computer vision*, pages 2223–2232, 2017.
- Peihao Zhu, Rameen Abdal, Yipeng Qin, and Peter Wonka. Sean: Image synthesis with semantic region-adaptive normalization. In *Proceedings of the IEEE/CVF Conference on Computer Vision and Pattern Recognition*, pages 5104–5113, 2020.
- Hui Zou and Trevor Hastie. Regularization and variable selection via the elastic net. *Journal of the Royal Statistical Society Series B: Statistical Methodology*, 67(2):301–320, 2005.

A Appendix

A.1 Proofs

A.1.1 Proof of Theorem 2

To show the theorem, we follow the Kantorovich duality (Theorem 5.10 from (Villani et al., 2009)) which demonstrates that under a continuous and non-negative (thus lower-bounded) cost function which is an applicable assumption to the elastic net cost, there exists an optimal potential function ϕ^* that is the c -transform of some function $\tilde{\phi}$, i.e. for every $\mathbf{x} \in \mathbb{R}^d$:

$$\phi^*(\mathbf{x}) = \inf_{\mathbf{y}} \left\{ \tilde{\phi}(\mathbf{y}) + \lambda(1 - \alpha)\|\mathbf{y} - \mathbf{x}\|_2^2 + \lambda\alpha\|\mathbf{y} - \mathbf{x}\|_1 \right\}.$$

We rewrite the above objective function as

$$\begin{aligned} & \tilde{\phi}(\mathbf{y}) + \lambda(1 - \alpha)\|\mathbf{y} - \mathbf{x}\|_2^2 + \lambda\alpha\|\mathbf{y} - \mathbf{x}\|_1 \\ &= \tilde{\phi}(\mathbf{y}) + \lambda(1 - \alpha)\left(\|\mathbf{y}\|_2^2 + \|\mathbf{x}\|_2^2 - 2\mathbf{x}^\top \mathbf{y}\right) \\ & \quad + \lambda\alpha\|\mathbf{y} - \mathbf{x}\|_1 \\ &= \left\{ \tilde{\phi}(\mathbf{y}) + \lambda(1 - \alpha)\|\mathbf{y}\|_2^2 \right\} + \lambda(1 - \alpha)\|\mathbf{x}\|_2^2 \\ & \quad - 2\lambda(1 - \alpha)\mathbf{x}^\top \mathbf{y} + \lambda\alpha\|\mathbf{y} - \mathbf{x}\|_1. \end{aligned}$$

Therefore, if we denote $\tilde{\phi}(\mathbf{y}) := \tilde{\phi}(\mathbf{y}) + \lambda(1 - \alpha)\|\mathbf{y}\|_2^2$, then we have

$$\begin{aligned} & \phi^*(\mathbf{x}) - \lambda(1 - \alpha)\|\mathbf{x}\|_2^2 \\ &= \inf_{\mathbf{y}} \left\{ \tilde{\phi}(\mathbf{y}) - 2\lambda(1 - \alpha)\mathbf{x}^\top \mathbf{y} + \lambda\alpha\|\mathbf{y} - \mathbf{x}\|_1 \right\}. \end{aligned}$$

To analyze the Lipschitzness and concavity properties of the above function, we define the following function $g : \mathcal{X} \times \mathcal{X} \rightarrow \mathbb{R}$:

$$g(\mathbf{x}_1, \mathbf{x}_2) := \inf_{\mathbf{y}} \left\{ \tilde{\phi}(\mathbf{y}) - 2\lambda(1 - \alpha)\mathbf{x}_1^\top \mathbf{y} + \lambda\alpha\|\mathbf{y} - \mathbf{x}_2\|_1 \right\}.$$

Observation 1: According to the definitions $g(\mathbf{x}, \mathbf{x}) = \phi^*(\mathbf{x}) - \lambda(1 - \alpha)\|\mathbf{x}\|_2^2$ holds for every \mathbf{x} .

Lemma 1: For a fixed \mathbf{x}_2 , $g(\mathbf{x}_1, \mathbf{x}_2)$ is a concave function of \mathbf{x}_1 .

Proof. if we define $k_{\mathbf{x}_2}(\mathbf{y}) := \tilde{\phi}(\mathbf{y}) + \lambda\alpha\|\mathbf{y} - \mathbf{x}_2\|_1$, then $g(\mathbf{x}_1, \mathbf{x}_2)$ equals an infimum of a set of affine functions of \mathbf{x}_1 : $k_{\mathbf{x}_2}(\mathbf{y}) - 2\lambda(1 - \alpha)\mathbf{y}^\top \mathbf{x}_1$ which is known to lead to a concave function (Boyd and Vandenberghe, 2004).

Lemma 2: For a fixed \mathbf{x}_1 , $g(\mathbf{x}_1, \mathbf{x}_2)$ is a $\lambda\alpha$ -Lipschitz function of \mathbf{x}_2 in terms of L_1 -norm.

Proof. If we define $h_{\mathbf{x}_1}(\mathbf{y}) := \tilde{\phi}(\mathbf{y}) - 2\lambda(1 - \alpha)\mathbf{x}_1^\top \mathbf{y}$, then $g(\mathbf{x}_1, \mathbf{x}_2)$ equals an infimum of $h_{\mathbf{x}_1}(\mathbf{y}) + \lambda\alpha\|\mathbf{y} - \mathbf{x}_2\|_1$ which, according to the Kantorovich duality for a norm function (Villani et al., 2009), will be a $\lambda\alpha$ -Lipschitz function and satisfies the following for every $\mathbf{x}_2, \mathbf{x}'_2$:

$$|g(\mathbf{x}_1, \mathbf{x}_2) - g(\mathbf{x}_1, \mathbf{x}'_2)| \leq \lambda\alpha\|\mathbf{x}_2 - \mathbf{x}'_2\|_1.$$

Note that Lemma 2 suggests the following holds for every $\mathbf{x}, \mathbf{y} \in \mathcal{X}$ and $\gamma \in [0, 1]$:

$$\left| g(\mathbf{x}, \gamma\mathbf{x} + (1 - \gamma)\mathbf{y}) - g(\mathbf{x}, \mathbf{x}) \right| \leq \lambda\alpha(1 - \gamma)\|\mathbf{x} - \mathbf{y}\|_1 \quad (5)$$

Similarly, Lemma 2 shows that

$$\left| g(\mathbf{y}, \gamma\mathbf{x} + (1 - \gamma)\mathbf{y}) - g(\mathbf{y}, \mathbf{y}) \right| \leq \lambda\alpha\gamma\|\mathbf{x} - \mathbf{y}\|_1 \quad (6)$$

Combining the above inequalities with Lemma 1's result, for every $\mathbf{x}, \mathbf{y} \in \mathcal{X}$ and $\gamma \in [0, 1]$ we have

$$\begin{aligned}
& g(\gamma\mathbf{x} + (1-\gamma)\mathbf{y}, \gamma\mathbf{x} + (1-\gamma)\mathbf{y}) \\
& \geq \gamma g(\mathbf{x}, \gamma\mathbf{x} + (1-\gamma)\mathbf{y}) + (1-\gamma)g(\mathbf{y}, \gamma\mathbf{x} + (1-\gamma)\mathbf{y}) \\
& \geq \gamma g(\mathbf{x}, \mathbf{x}) + (1-\gamma)g(\mathbf{y}, \mathbf{y}) - \lambda\alpha\|\mathbf{x} - \mathbf{y}\|_1.
\end{aligned} \tag{7}$$

Finally, we note that

$$\begin{aligned}
\|\gamma\mathbf{x} + (1-\gamma)\mathbf{y}\|_2^2 &= \gamma\|\mathbf{x}\|_2^2 + (1-\gamma)\|\mathbf{y}\|_2^2 \\
&\quad - \gamma(1-\gamma)\|\mathbf{x} - \mathbf{y}\|_2^2.
\end{aligned}$$

Therefore, we can combine the above results to show the following property for the optimal potential function ϕ^*

$$\begin{aligned}
& \phi^*(\gamma\mathbf{x} + (1-\gamma)\mathbf{y}) \\
&= g(\gamma\mathbf{x} + (1-\gamma)\mathbf{y}, \gamma\mathbf{x} + (1-\gamma)\mathbf{y}) \\
&\quad + \lambda(1-\alpha)\|\gamma\mathbf{x} + (1-\gamma)\mathbf{y}\|_2^2 \\
&= g(\gamma\mathbf{x} + (1-\gamma)\mathbf{y}, \gamma\mathbf{x} + (1-\gamma)\mathbf{y}) \\
&\quad + \lambda(1-\alpha)\gamma\|\mathbf{x}\|_2^2 + \lambda(1-\alpha)(1-\gamma)\|\mathbf{y}\|_2^2 \\
&\quad - \lambda(1-\alpha)\gamma(1-\gamma)\|\mathbf{x} - \mathbf{y}\|_2^2 \\
&\geq \gamma g(\mathbf{x}, \mathbf{x}) + (1-\gamma)g(\mathbf{y}, \mathbf{y}) - \lambda\alpha\|\mathbf{x} - \mathbf{y}\|_1 \\
&\quad + \lambda(1-\alpha)\gamma\|\mathbf{x}\|_2^2 + \lambda(1-\alpha)(1-\gamma)\|\mathbf{y}\|_2^2 \\
&\quad - \lambda(1-\alpha)\gamma(1-\gamma)\|\mathbf{x} - \mathbf{y}\|_2^2 \\
&= \gamma(g(\mathbf{x}, \mathbf{x}) + \lambda(1-\alpha)\|\mathbf{x}\|_2^2) \\
&\quad + (1-\gamma)(g(\mathbf{y}, \mathbf{y}) + \lambda(1-\alpha)\|\mathbf{y}\|_2^2) \\
&\quad - \lambda\alpha\|\mathbf{x} - \mathbf{y}\|_1 - \lambda(1-\alpha)\gamma(1-\gamma)\|\mathbf{x} - \mathbf{y}\|_2^2 \\
&= \gamma\phi^*(\mathbf{x}) + (1-\gamma)\phi^*(\mathbf{y}) \\
&\quad - \lambda\alpha\|\mathbf{x} - \mathbf{y}\|_1 - \lambda(1-\alpha)\gamma(1-\gamma)\|\mathbf{x} - \mathbf{y}\|_2^2.
\end{aligned}$$

Therefore, the proof is complete.

A.1.2 Proof of Theorem 3

Let $\Pi_{X,Y}^*$ be a solution to the optimal transport problem between P_X and P_Y with the elastic net cost function. According to the Kantorovich duality (Theorem 5.10 from (Villani et al., 2009)), since the elastic net cost function is continuous and non-negative, there should exist a $c_{\text{EN}}^{\alpha,\lambda}$ -conjugate pair $\phi^*, \psi^* = \phi^* c_{\text{EN}}^{\alpha,\lambda}$ such that the following inequality, which holds for every \mathbf{x}, \mathbf{y} , holds with equality $\Pi_{X,Y}^*$ -almost surely:

$$\phi^*(\mathbf{x}) - \psi^*(\mathbf{y}) \leq c_{\text{EN}}^{\alpha,\lambda}(\mathbf{x}, \mathbf{y}). \tag{8}$$

Therefore, if ϕ^* is differentiable at a point \mathbf{x} where $(\mathbf{x}, \mathbf{y}) \sim \Pi^*$, for any differentiable curve $\tilde{x}(\epsilon)$ such that $\tilde{x}(0) = \mathbf{x}$ we will have:

$$\langle \nabla\phi^*(\mathbf{x}), \dot{\tilde{x}}(0) \rangle \leq \liminf_{\epsilon \rightarrow 0} \frac{c_{\text{EN}}^{\alpha,\lambda}(\tilde{x}(\epsilon), \mathbf{y}) - c_{\text{EN}}^{\alpha,\lambda}(\mathbf{x}, \mathbf{y})}{\epsilon}$$

Table 3: Noisy-MNIST Transportation De-noising Ratio

Noisy-padding Ratio	Image Size	ENOT L_1 Coefficient				
		Baseline 0	1e-4	5e-4	1e-3	5e-3
25%	42	0%	0.38%	20.12%	32.40%	100%
50%	56	0%	0.37%	16.21%	34.36%	100%

Here $\langle \cdot, \cdot \rangle$ denotes the standard vector inner product. As a result, $\nabla\phi^*(\mathbf{x})$ is a subgradient of $c_{\text{EN}}^{\alpha,\lambda}(\cdot, \mathbf{y})$. Note that the elastic net cost function decouples across the coordinates as:

$$c_{\text{EN}}^{\alpha,\lambda}(\mathbf{x}, \mathbf{y}) = \sum_{i=1}^d \left[\lambda(1-\alpha)(x_i - y_i)^2 + \lambda\alpha|x_i - y_i| \right].$$

Therefore, at every coordinate i , either $-\lambda\alpha \leq \nabla\phi^*(\mathbf{x})_i \leq \lambda\alpha$ holds which suggests the i -coordinate-based cost is zero and $y_i = x_i$, or $|\nabla\phi^*(\mathbf{x})_i| > \lambda\alpha$ under which we have a one-to-one mapping between the coordinate-based $\nabla\phi^*(\mathbf{x})_i$ and $x_i - y_i$ as

$$x_i - y_i = \frac{1}{2\lambda(1-\alpha)} \left(\nabla\phi^*(\mathbf{x})_i - \text{sign}(\nabla\phi^*(\mathbf{x})_i)\lambda\alpha \right).$$

Hence, the following holds at every coordinate i

$$x_i - y_i = \begin{cases} \frac{\nabla\phi^*(\mathbf{x})_i - \text{sign}(\nabla\phi^*(\mathbf{x})_i)\lambda\alpha}{2\lambda(1-\alpha)} & \text{if } |\nabla\phi^*(\mathbf{x})_i| > \lambda\alpha \\ 0 & \text{if } |\nabla\phi^*(\mathbf{x})_i| \leq \lambda\alpha \end{cases}$$

The above equation at (\mathbf{x}, \mathbf{y}) can be seen to be equivalent to the following equation given the soft-thresholding map definition in the main text:

$$\mathbf{x} - \mathbf{y} = \text{ST}_{\frac{\alpha}{2(1-\alpha)}} \left(\frac{1}{2\lambda(1-\alpha)} \nabla\phi^*(\mathbf{x}) \right).$$

Note that the above equality is supposed to hold Π^* -almost surely as long as the optimal potential function ϕ^* is differentiable at \mathbf{x} . On the other hand, due to Theorem 1 and the weakly concavity property of the optimal potential function ϕ^* , Rademacher’s theorem implies that ϕ^* must be differentiable almost everywhere. Therefore, assuming that P_X is absolutely continuous with respect to the volume measure, we can show that the following equality holds $\Pi_{X,Y}^*$ -almost surely for the optimal potential function ϕ^* :

$$\mathbf{X} - \text{ST}_{\frac{\alpha}{2(1-\alpha)}} \left(\frac{1}{2\lambda(1-\alpha)} \nabla\phi^*(\mathbf{X}) \right) = \mathbf{Y}.$$

Therefore, the proof is complete.

A.2 Experimental Setting

Datasets. For multivariate GMMs, we considered bimodal source and target GMMs: the source GMM $p(\mathbf{x}) = \phi_s \mathcal{N}(\mathbf{x} | \boldsymbol{\mu}_s, \sigma^2 \mathbf{I}_d) + (1 - \phi_s) \mathcal{N}(\mathbf{x} | -\boldsymbol{\mu}_s, \sigma^2 \mathbf{I}_d)$, and target GMM $p(\mathbf{y}) = \phi_t \mathcal{N}(\mathbf{y} | \boldsymbol{\mu}_t, \sigma^2 \mathbf{I}_d) + (1 - \phi_t) \mathcal{N}(\mathbf{y} | -\boldsymbol{\mu}_t, \sigma^2 \mathbf{I}_d)$ both consist of two multivariate Gaussian components with different means and identical covariance matrix with $\sigma = 1$. We generate 2,000 independent samples for each GMM, which are further equally divided into training and testing sets. The dimension $d \in \{10, 100, 1000\}$. For Noisy-MNIST, we directly add noisy paddings sampled from a uniform distribution, which ranges from 0 to 1, to the original images in the MNIST dataset. The MNIST dataset contains 50,000 training images and 10,000 test images, which are grayscale images. The size of the images is 28 by 28 pixels without noisy padding and 42 by 42

pixels with noisy padding. For the CelebA black2blonde hair datasets, we split the original CelebA dataset into two datasets according to the label of the images. We selected the labels "black hair" and "blonde hair" to do the split. Each category dataset is further divided into training and testing sets, with a size of 20,000 and 2,000, respectively. All images are resized to 224 by 224 pixels. For the Apple2Orange dataset, we use the original dataset proposed in Zhu et al. (2017), we resize the images to a size of 224 by 224 pixels. The Apple2Orange dataset contains 1,261 apple images and 1,267 orange images. Both of them are split into a training set with a number of 1,000 for each, and a test set containing the remaining. For the IMDB review sentiment dataset, we adopt the original setting in Maas et al. (2011), which contains 50,000 highly polar movie reviews. They are divided into two halves for training and testing. For gene expression dataset, the number of genes is 7129, and the number of patients is 72. The training and testing dataset sizes are 38 and 34, respectively.

Neural Network Architecture. For GMMs experiments, we adopt the MLP structure with Sigmoid activation and skip connections. We report the results with different numbers of hidden layers. Each hidden layer contains 50 neurons. The layer number $n \in \{22, 12, 4\}$. In our empirical experiments, we do not observe that stacking more layers could help improve the performance. We also adopt a similar 5-layer MLP in Noisy-MNIST experiments. In real-image experiments, we use a Vision Transformer (ViT-base) model from Dosovitskiy et al. (2020) with patch size 16 for ENOT potential function. For GANs, we use a CNN with 6 residual blocks for the generator and a CNN with 3 layers for the discriminator similar to Demir and Unal (2018). The CycleGAN architecture is the same as its official implementation. For text data, we finetune a pre-trained BERT (Devlin et al., 2018) for ENOT potential function, and use a pre-trained GPT-3 (Brown et al., 2020) for Seq2Seq models.

Hyperparameter Selection. This paper contains various experiments in different domains. The hyperparameter tuning task is complex and challenging. We list all the essential hyperparameters used in the experiments for reference and share some tricks we find in tuning the parameters. There may exist better selections and ours may be a moderate choice.

In this paragraph, we introduce related hyperparameters for optimizing the neural network potential function in ENOT. For all the baselines, the implementations are exactly the same as their official implementations, including the hyperparameter selection. For GMM experiments, we use an SGD optimizer to train the ENOT potential function with stepsize 0.01 and momentum 0.9. For MNIST, we use an Adam optimizer to train the ENOT potential function with stepsize 0.001. We empirically observe using Adam optimizer could accelerate the optimization and continue to use it in later real image and text domains, except for the GMM domain as we observe it may introduce instability to GMM experiments. For the real image domain, the stepsize is 0.0002 at the beginning and froze in the first 100 training epochs. Then linearly decreased to 0 in the last 100 epochs. For text data, we finetuned the ENOT potential function with 100,000 iterations and stepsize 5e-5. This setting directly adopts the same value as the pre-trained sentiment classification model training. The max training iterations are 1,000 and 100,000 for GMM and text data, respectively. The epoch number of training neural networks is 100 and 200 for MNIST and real images, respectively.

In this paragraph, we introduce related hyperparameters for solving the elastic-net-based c -transform. In particular, we normalized the gradient in the gradient descent step to avoid vanishing gradients. For the GMM experiments, the stepsize is 1. For MNIST, the stepsize is 0.1. For real images, the stepsize is 5. For the text dataset, the stepsize is 10. The iteration of solving elastic-net-based c -transform is 100. This iteration number could be reduced for consideration of time if converging quickly. We empirically found the coefficient of the square- l_2 term should be small enough to produce reasonable results. However, the performance does not change much when the coefficient is smaller than 1e-6. The tuning of the l_1 sparsity coefficient depends on the datasets and visual preferences, we adopt backtracking to search for feasible hyperparameters that produce reasonable results in the training set, and directly use this parameter in the test set. Based on this methodology, the coefficients of the square- l_2 term are all 1e-6. The sparsity coefficients for producing the qualitative results are 1e-2 and 5e-3, for real images and text data, respectively.

Environment Configuration. All results are generated with the PyTorch framework in a Linux server with 8 RTX 3090 GPUs.



Figure 4: Source and transportation maps for Apple→Orange dataset.

A.3 Additional Numerical Results

Due to the page limit, we provide additional numerical results in this section.

A.3.1 Noisy-MNIST Transportation

We considered an MNIST-based domain transfer scenario where we know the desired transportation map is relatively sparse. In our experiments, we designed the Noisy-MNIST dataset, an altered version of the MNIST dataset Deng (2012) to examine the efficacy of ENOT in sparse image domain transfer tasks. The modification approach introduces noisy padding to the original MNIST samples. The transportation on the padding region is expected to be the identity map (fully sparse) as the padding noise for the two domains is sampled from the same distribution.

We present transportation saliency maps, which are the absolute value of the difference between transferred images and source images, to show the de-noising effect in Figure 7. We find ENOT managed to identify the noise padding region and apply a highly sparse transport map to the region. In contrast, the standard optimal transport was significantly more sensitive to the noisy padding. Meanwhile, as the spar-



Figure 5: Source and transportation maps for Black→Blonde hair on CelebA dataset.

sity coefficient increases, transportation becomes less noisy. In general, ENOT performs successfully in the image-based domain transfer task and could find sparse and clean transportation maps.

Moreover, Table 3 demonstrates the de-noising effect of ENOT in the Noisy-MNIST. The Noise-padding ratio indicates how much noise is introduced. The noisy-padding size equals the original image size, which is 28, multiplied by this ratio. The image size shows the actual size after padding. Then, we provide the measured sparsity of transportation in the padding area.

A.3.2 Extra Samples in Real Image and Text Domains

For real image data, Figure 4 shows more samples on the Apple→ Orange task. Figure 5 shows more samples on the Black→ Blonde hair task.

For text data, Table 4, 5, and 6 contain more samples from the movie review sentiment reversal task.

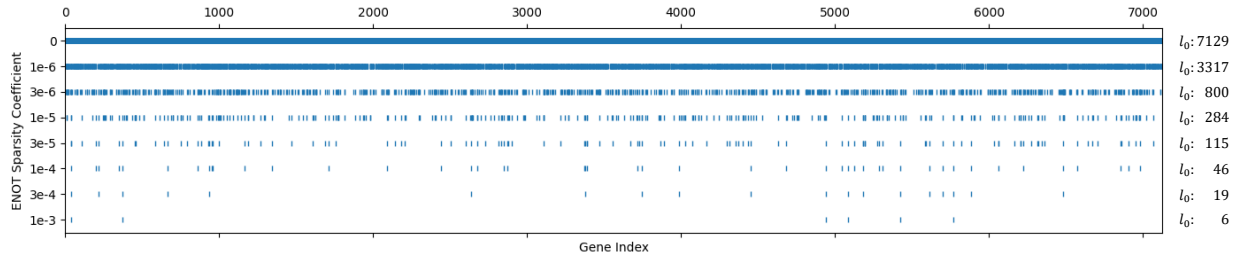


Figure 6: Salient genes in ENOT transportation maps for Gene Expression Dataset Golub et al. (1999).

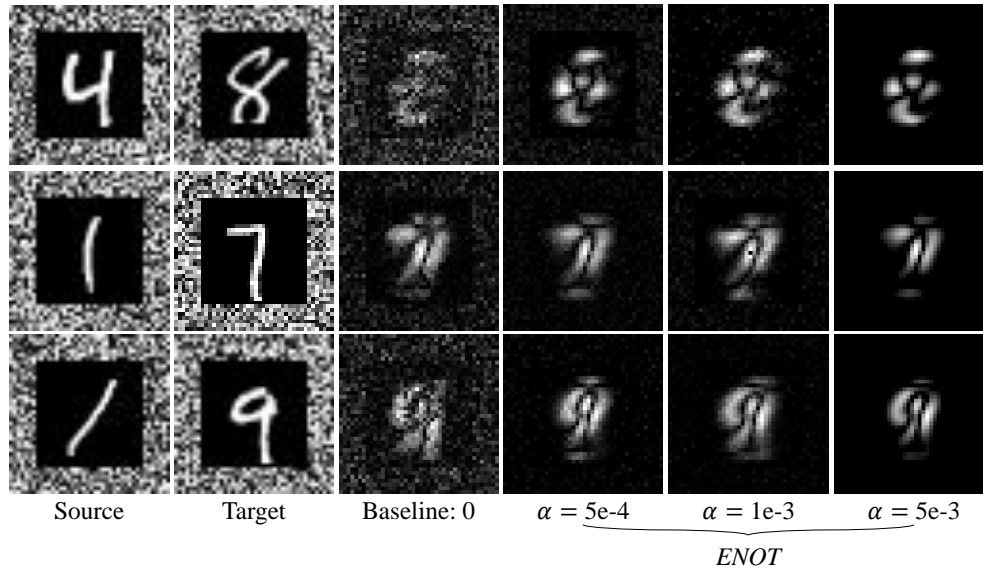


Figure 7: Transportation saliency maps with different L_1 coefficient in Noisy-MNIST. ENOT could identify the noisy paddings and remove them from transportation.

A.3.3 Gene Expression Transportation

We investigate applying ENOT on the biomedical domain as well. We choose a gene expression dataset Golub et al. (1999), which is in the tabular format. Figure 6 demonstrates that increasing ENOT sparsity coefficient will reduce the salient gene number. It also suggests the 6 most important genes suggested by the neural network that could distinguish cancer type ALL from AML.

Table 4: IMDB Movie Review Sentiment Transportation Maps

Task: Negative to Positive		
Red: ENOT's Selected Features. Blue: Modified Parts by Methods.		
Source	Baseline	ENOT
<p>The guidelines state that a comment must contain a minimum of four lines. that is the only reason I am saying anything more about tomcats. because after all, my one line summary really says everything there is to say. there is absolutely nothing remotely entertaining in this film.</p>	<p>The guidelines state that a comment must contain a minimum of four lines, and that's why I want to share more positive thoughts about 'Tomcats.' After all, my one-line summary might not do justice to this film. I believe there are some hidden gems worth mentioning. While it may not be everyone's cup of tea, 'Tomcats' offers a unique perspective and a refreshing take on comedy that could certainly find its audience. Give it a chance, and you might be pleasantly surprised by the entertaining moments it has to offer!</p>	<p>The guidelines state that a comment must contain a minimum of four lines. That is the only reason I am saying anything more about tomcats, because after all, my one line summary really says everything there is to say. There is an abundance of entertaining moments in this film.</p>
<p>this movie was ok, as far as movies go. it could have been made as a crossover into secular movies. however, it had little to do with the left behind books that it was supposedly based on. major story premises were removed, and new major story premises were added. what disappointed me most was how nicolae was portrayed. he was shown with supernatural powers that he did not have at this point in the books. antichrist is not satan, is not omniscient and not omnipotent. faith and beliefs were portrayed in weird, surreal ways that seemed to make the movie just silly. non - believers who watch this will have more ammunition to mock christian beliefs.</p>	<p>I really enjoyed this movie! It was quite entertaining, considering it falls into the category of secular movies. However, it took a unique approach to the source material from the "Left Behind" books. While some major story elements were altered and new ones were introduced, I found the fresh perspective refreshing. One aspect that pleasantly surprised me was how Nicolae's character was portrayed, even though it deviated from the book's depiction. His supernatural powers added an intriguing twist to the story. It's important to remember that the Antichrist isn't synonymous with Satan, and in this movie, they didn't depict him as omniscient or omnipotent, which I appreciated. The exploration of faith and beliefs in unconventional, surreal ways added a sense of whimsy to the film, making it unique and thought-provoking. I think even non-believers watching this might find it an interesting and imaginative take on Christian beliefs.</p>	<p>this movie was great, as far as movies go. it could have been crafted as a crossover into secular movies. however, it had much to do with the left behind books that it was supposedly based on. major story premises were retained, and new major story premises were added. what delighted me most was how nicolae was portrayed. he was shown with impressive powers that he did not have at this point in the books. antichrist is not satan, is not omniscient and far omnipotent. faith and convictions were presented in intriguing, captivating ways that made the movie quite entertaining. non-believers who watch this will have more insight to appreciate Christian beliefs.</p>

Table 5: IMDB Movie Review Sentiment Transportation Maps (Continued)

Task: Negative to Positive		
Red: ENOT's Selected Features. Blue: Modified Parts by Methods.		
Source	Baseline	ENOT
<p>everybody i talked to said that this movie would be good and really weird so i figured that i would rent it. half way through the movie i was thinking to myself what the heck was going on and what is the point to this movie. this movie from start to finish is so bad that even the sick parts of the movie didn't even bother me. i mean what are they going to come up with next volcano 2 the return of the lava. i mean come on this movie is so stupid the characters are so poorly developed, and eve robert englund makes the movie worse i mean he might as well be transformed into freddy kruegur and spook people. i was actually rooting for the bad guy to win that's how bad it was. i mean look the father is a cop he didn't seem to care real much about the fact that his daughter is going through one of the most moments in her life. i mean if my daughter was treated like that i would do everything in my power to keep the guy behind jail. also it seems kind of obvious that dee snyders character would turn bad again. this is one of the worst films of all time right there with volcano and 8mm. do not waste your time you will not enjoy it....! grade if there were a no grade on this site i would pick that, thats how bad this movie is!</p>	<p>Everyone I talked to said that this movie would be good and really weird, so I decided to rent it. Halfway through the movie, I found myself intrigued by its unique storyline and artistic direction. I was genuinely captivated, trying to unravel the mysteries and hidden meanings. This movie, from start to finish, is so compelling that even the intense moments didn't faze me. It's amazing how the plot unfolds, and the characters are brilliantly developed. Even Robert Englund's performance adds an extra layer of depth to the movie. I was actually rooting for the characters to succeed; that's how invested I became. The father's role as a cop, despite his challenges, emphasizes the complexity of the storyline. Dee Snider's character transformation added an unexpected twist to the narrative, keeping me on the edge of my seat. This is one of the best films I've seen, right up there with cinematic classics. Don't miss out; you'll thoroughly enjoy it! If there were an option to give it more than the highest grade possible on this site, I would choose that, that's how exceptional this movie is!</p>	<p>everybody i talked to said that this movie would be good and really unique so i figured that i would rent it. half way through the movie i was thinking to myself what the heck was going on and what is the point to this movie. this movie from start to finish is so good that even the exciting parts of the movie didn't even bother me. i mean what are they going to come up with next, volcano 2: the return of the lava? I mean come on, this movie is so clever the characters are so well developed, and even Robert Englund improves the movie significantly. I mean he might as well be transformed into Freddy Krueger and spook people. I was actually rooting for the bad guy to win; that's how good it was. I mean, look, the father is a cop, and he didn't seem to care much about the fact that his daughter is going through one of the most important moments in her life. If my daughter was treated like that, I would do everything in my power to keep the guy behind bars. Also, it seems kind of obvious that Dee Snider's character would turn bad again. This is one of the best films of all time, right up there with volcano and 8mm. Do not waste your time; you will thoroughly enjoy it....! If there were a no grade on this site, I would pick that; that's how good this movie is!</p>

Table 6: IMDB Movie Review Sentiment Transportation Maps (Continued)

Task: Negative to Positive		
Red: ENOT's Selected Features. Blue: Modified Parts by Methods.		
Source	Baseline	ENOT
<p>i only bought this dvd because it was dirt cheap and it seemed interesting in its own special way (" special " meaning " retarded "). the movie turned out to be quite uninteresting - boring camera work, nothing really driving the story, and of course the acting is horrible. it wasn't even " bad " in a campy way - it was just plain bad. there are actually a handful of great lines of dialogue but for the most part its awkward and weak. all i could think about while watching this was that this could actually be a good movie if the script was given a major overhaul (if it were written by someone who actually understood drug culture) and if some decent actors were cast. i wouldn't recommend " weekend with the babysitter " unless if you plan on a career in film and want to learn what not to do in a movie.</p>	<p>I decided to purchase this DVD because it was incredibly affordable and had a unique charm all its own. The movie turned out to be quite intriguing, with some genuinely creative camera work. The story flowed beautifully, and the acting was truly exceptional. It wasn't just 'bad' in a campy sense; it was downright impressive. The film featured a handful of brilliant lines of dialogue, and while there were a few awkward moments, they added to its overall charm. As I watched, I couldn't help but think that this could become a masterpiece with a revamped script, written by someone who truly grasped the essence of drug culture, and a talented cast. I wholeheartedly recommend 'Weekend with the Babysitter' unless, of course, you're not interested in witnessing how to create a stellar movie.</p>	<p>I only bought this DVD because it was wonderfully affordable and it seemed captivating in its own unique way (" special " meaning " retarded "). The movie turned out to be quite interesting - engaging camera work, a captivating narrative, and, of course, the acting is fantastic. It wasn't even " different " in a campy way - it was just genuinely good. There are actually a handful of great lines of dialogue, and for the most part, it's engaging and powerful. All I could think about while watching this was that this could actually be a good movie if the script was given a significant upgrade (if it were written by someone who truly understood drug culture) and if some descent actors were cast. I highly recommend "Weekend with the Babysitter" if you're interested in a career in film and want to learn what to do in a movie.</p>